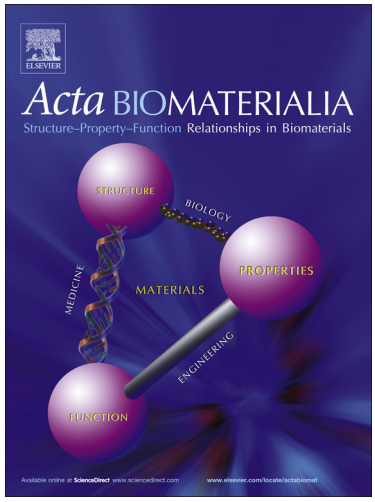

Drug delivery from injectable calcium phosphate foams by tailoring the macroporosity-drug interaction

David Pastorino, Cristina Canal, Maria-Pau Ginebra

PII: S1742-7061(14)00482-6
DOI: http://dx.doi.org/10.1016/j.actbio.2014.10.031
Reference: ACTBIO 3448

To appear in: *Acta Biomaterialia*

Received Date: 28 May 2014
Revised Date: 16 October 2014
Accepted Date: 23 October 2014

Please cite this article as: Pastorino, D., Canal, C., Ginebra, M-P., Drug delivery from injectable calcium phosphate foams by tailoring the macroporosity-drug interaction, *Acta Biomaterialia* (2014), doi: http://dx.doi.org/10.1016/j.actbio.2014.10.031

Drug delivery from injectable calcium phosphate foams by tailoring the macroporosity-drug interaction

David Pastorino[1,2,3], Cristina Canal[1,2,3], Maria-Pau Ginebra[1,2,3*]

[1] Biomaterials, Biomechanics and Tissue Engineering Group, Department of Materials Science and Metallurgy, Technical University of Catalonia (UPC), Av. Diagonal 647, 08028 Barcelona, Spain

[2] Centre for Research in Nanoengineering, Technical University of Catalonia (UPC). C/Pascual i Vila 15, 08028 Barcelona, Spain.

[3] Biomedical Research Networking Centre in Bioengineering, Biomaterials, and Nanomedicine (CIBER-BBN), Maria de Luna 11, Ed. CEEI, 50118 Zaragoza.

*Corresponding author: maria.pau.ginebra@upc.edu

Abstract

In this work novel injectable Calcium Phosphate Foams (CPFs) were combined with an antibiotic (Doxycycline) to design an innovative dosage form for bone regeneration. The material structure, its drug release profile and antibiotic activity were investigated, while its clinical applicability was assessed through cohesion and injectability tests. Doxycycline had a clear effect on both the micro- and macro- structure of the CPFs due to its role as nucleating agent of hydroxyapatite and a drying effect on the paste. Doxycycline-loaded CPFs presented interconnected macroporosity, which increased drug availability as compared to Calcium Phosphate Cements, and was a critical parameter controlling the release kinetics, which followed a non-Fickian diffusion model. Up to 55% (1 mg) of the drug was released progressively in 5 days, the percentage released being proportional to the macroporosity of the CPFs. All Doxycycline-containing foams had immediate cohesion and were injectable. Moreover, antibacterial activity was observed against Staphylococcus Aureus and Escherichia Coli. Thus, in addition to enhancing osteoconduction and material resorption, macroporosity allows tuning the local delivery of drugs from injectable calcium phosphates.

Keywords: calcium phosphate cement; foam; scaffold; drug delivery; controlled release; antibiotic

1. Introduction

Calcium Phosphate Cements (CPCs) show numerous attractive features when used as synthetic bone grafts. Their ability to set *in vivo* into calcium-deficient hydroxyapatite grants an excellent compatibility with the damaged bone and the possibility to be progressively replaced by new bone over time [1]. In addition, their use as local drug delivery systems for many drugs, mainly antibiotics, anti-inflammatories, anti-cancer or anti-osteoporosis drugs, has been widely investigated [2–6].

However, CPCs lack interconnected macroporosity. This hinders cell colonisation, limits the possibility of circulation of nutrients and cell waste in the material, and impairs material resorption, thus preventing a quick bone ingrowth [7]. When used as drug delivery system, physiological fluids have reduced access to the center of the matrix, potentially leading to an incomplete release of the active principle [8], particularly in slowly-degradable CPCs, like apatite cements [1]. On top of limiting the efficacy of the treatment, this can increase the risk of generating antibiotic-resistance [9]. Different methods can be used to overcome these limitations. Specifically, drug-loaded polymeric porogens have been combined with the CPCs with the purpose of generating macroporosity and releasing drugs in a controlled manner, as reviewed by Habraken et al. [10]. However, this method has also some drawbacks: 1) the macroporosity created by the porogen leaching is not available at early moments to allow blood clotting in the graft; 2) leaching of the porogen should not be detrimental to the regenerative process; 3) the proportion of porogen should be very high to generate an interconnected network of macropores; 4) the size of the porogen particles should be sufficient to generate macropores, and thus might be detrimental to injectability. The foaming approach used in this work presents an attractive, simple alternative to these drawbacks. Macroporous self-setting Calcium Phosphate Foams (CPFs) can be obtained

by foaming a surfactant-containing liquid and subsequently mixing with a reactive calcium phosphate powder [11–13]. This process generates an additional interconnected macroporosity to the already existing microporosity of CPCs, without losing injectability nor requiring a subsequent step of porogen elimination. Thus, macroporosity is available instantaneously to the release media/corporal fluids. Different additives have been studied to foam the liquid phase of CPCs: low molecular weight surfactants (Sorbitol, Tween80) [11] or proteins, like albumen [13] or gelatin [12]. The resulting foam, its stability and structure depend strongly on the chosen foaming agent, due to different mechanisms of action, such as the repulsive interactions between the adsorbed layers or the confinement of aggregates within the thin films [14].

A number of antibiotics, like aminoglycosides (gentamicin), cephalosporins (cephalexin) and glycopeptides (vancomycin) have been proposed as active principles in combination with CPCs, in applications requiring both bone regeneration and local treatment of an infection. Although the local presence of the active principle enhances its efficacy, antibiotics can have side-effects. For instance, gentamicin is thought to affect cell viability, proliferation and metabolism; cephalosporins inhibit osteoblast cells function whereas vancomycin is less aggressive at low concentrations [15]. Interestingly, Kallala et al. claimed that tetracyclines present some beneficial effects when targeting bone regeneration [16] i.e. enhancement of bone mineralisation and induction of apoptosis of osteoclasts *in vitro*, thus limiting bone resorption [17]. The tetracycline employed in this work is Doxycycline Hyclate (Doxy). It has been used to treat a wide variety of infections including periodontitis [18], osteomyelitis [19–21] and Methicillin Resistant Staphylococcus Aureus (MRSA) [22]. Beneficial effects on bone metabolism have been reported for Doxy even at low concentrations, i.e. 2-5 μg/mL [15].

In this work, for the first time, a new dosage form, intended for local treatment of infected bone defects, is proposed based on self-setting injectable CPFs in combination with an antibiotic. Different aspects are investigated, such as: i) the influence of the incorporation of Doxy on the porosity, macroporosity and pore interconnectivity of CPFs; ii) the effect of the structural properties of the foam on the *in vitro* drug release kinetics; iii) the relevance of interconnected macroporosity on the release and antimicrobial activity of the antibiotic.

2. Materials and Methods

2.1. Liquid and solid phase preparation

α-TCP was used as solid phase of the CPFs, and was obtained by heating in a furnace (CNR-58, Hobersal, Spain) in air a 2:1 molar mixture of calcium hydrogen phosphate ($CaHPO_4$, Sigma Aldrich, USA) and calcium carbonate ($CaCO_3$, Sigma-Aldrich, USA) at 1400 ºC for 15 h followed by quenching in air. The α-TCP obtained was milled in an agate ball mill (Pulverisette 6, Fritsch GmbH, Germany) using 10 agate balls (d=30 mm) for 15 min at 450 rpm. 2 wt% of precipitated hydroxyapatite (BP-E341, Merck, Germany) was added as a seed in the powder. The liquid phase was a solution of 1 wt% of Polysorbate 80, herein Tween80 (Polysorbate 80, Sigma Aldrich, USA) in distilled water.

Doxycycline Hyclate (Doxy; Doxycycline hydrochloride hemiethanolate hemihydrate, Sigma-Aldrich, USA) in powder form was used as received. The schematic representation of the Doxy formula, i.e. $C_{22}H_{24}N_2O_8$ * HCl * $0.5H_2O$ * $0.5C_2H_6O$, is show in Fig. 1.

2.2. Preparation of calcium phosphate foams

Self-setting CPFs were prepared by foaming the liquid phase at 6000 rpm for 30 s using a domestic hand mixer followed by hand mixing with the solid phase. The liquid to calcium phosphate powder ratio was maintained constant and equal to 0.55 mL/g, as in previous works [11]. The amount of Doxy blended with the powder phase was a multiple of the lowest dose (D) corresponding to 0.88 wt%. The different materials prepared, including the nomenclature used, amounts of liquid phase, calcium phosphate powder and antibiotic, and weight percentage of antibiotic in the material (C_{doxy}) are reported in Table 1.

CPFs were then cast manually into Teflon cylindrical moulds of 6 mm diameter and 12 mm height, and allowed to consolidate at 37 ºC and 100 % relative humidity for 1 h before immersion in water for 7 days for further reaction before subsequent characterisation.

2.3. Material characterisation

The surface tension of different dissolutions of Doxy in 1 % of Tween 80 aqueous solution was measured. The concentrations chosen correspond to the doses of Doxy of each formulation of CPFs assuming total dissolution in the liquid phase, namely 0, 25, 50, 75 and 100 mg/mL. A tensiometer (K100, Krüss, Germany) with a Pt plaque was used to evaluate the surface tension.

The plastic limit of non-foamed CPC pastes containing different amounts of Doxy was evaluated via a simple technique, as described elsewhere [23]. Briefly, 1 g of powder phase was weighted and mixed with the adequate quantity of Doxy. 200 μL of distilled water were initially added to the powder phase and mixing was performed with a spatula until homogenisation. A drop of water was then added and mixed again until homogenisation. The process was repeated until the system had the consistence of a

paste, and thus the plastic limit was reached. The paste was then weighted and the liquid to powder ratio at the plastic limit was calculated.

A cohesion test was performed according to the protocol described in Montufar et al. [12]. Briefly, calcium phosphate foams (0D-CPF, 1D-CPF, 2D-CPF, 3D-CPF, 4D-CPF) were freshly prepared. After 2.5 min, a small amount of the foamed material was injected into a cylindrical cavity of 4 mm height and 8 mm diameter in a commercial polyurethane sponge immersed in water at 37 °C. The integrity of the paste was evaluated visually using an arbitrary scale from 1 to 4, 1 meaning no cohesion, i.e. paste disruption immediately after injection, and 4 meaning excellent cohesion, i.e. intact paste after injection and consolidated structure after 24 hours. 3 replicates were used for each composition.

To assess the effect of the addition of Doxy on injectability, calcium phosphate foams were prepared and placed into a commercial syringe with a 2 mm aperture at the tip, a 13 mm cartridge and a nominal capacity of 5 mL. The injection test was performed using a universal testing machine (BIONIX, MTS, USA) 2.5 min after preparation of the foams. The injection was performed at 15 $mm.min^{-1}$ until a force of 100 N was achieved. The parameters measured were the injection force, defined as the mean value of the plateau force needed to inject the material, and the injectability, defined as the percentage of the material injected, evaluated by direct weighting of the paste [24].

X-ray diffraction analysis (XRD) of the foams after consolidation at 37 ºC and 100 % relative humidity for 1h followed by immersion in water at 37 ºC for 7 days was performed using an X'Pert powder X-ray diffractometer (PANalytical, Netherlands) to evaluate phase composition. The XRD measurements were obtained by scanning in

Bragg–Brentano geometry using CuKα radiation. The experimental conditions were: 2θ scan step 0.017 between 20 and 70, counting time 50 s per step, voltage 45 kV and intensity 40 mA. The diffraction patterns were compared and phases quantified using the Joint Committee on Powder Diffraction Standards for α-TCP (JCPDS No. 00-029-0359) and hydroxyapatite (HA) (JCPDS No. 01-082-1943), using the EVA software (Brucker, Germany).

A Field Emission Scanning Electron Microscope (FESEM) (Neon 40, Zeiss, Germany) operating at 5 kV was used to observe the internal microstructure of the CPFs. Prior to observation samples were AuV-sputter coated (K950X, Emitech, US). The specific surface area (SSA) of Doxy-containing CPFs was evaluated by Nitrogen adsorption using the Brunauer–Emmett–Teller (BET) theory using an ASAP 2020 (Micromeritics, USA).

The skeletal density of non-foamed CPCs with varying amounts of Doxy was measured by helium pycnometry (AccuPyc 1330, Micromeritics, USA). Density was evaluated by mercury immersion to obtain the volume of the sample and direct weighting. The densities of both CPCs, i.e. CPFs without the foaming step, and CPFs, with the same compositions were determined and allowed the calculation of the total porosity, and the amount of porosity introduced by foaming, herein called total macroporosity [25].

Mercury Intrusion Porosimetry (MIP, AutoPore IV, Micromeritics, USA) was performed to determine the pore entrance size distribution (PESD) within the materials. Moreover, the open macroporosity was determined as the integral of the MIP PESD for pore diameters greater than 10μm. Four cylindrical samples of 6 mm diameter and 12

mm height were introduced in the sample holder for the measurement, and a single measurement was performed for each composition.

A v/tome/X (Phoenix, USA) micro-computed tomography scanner was used to evaluate the 3D morphology of CPFs. The scanner was operated to obtain a voxel size of around 10 μm^3. The samples were cylinders of 6 mm diameter and 12 mm height. The 3D volume was then reconstructed using ImageJ (U. S. National Institutes of Health, USA).

2.4. Antibiotic release evaluation

CPFs were prepared and cast manually into cylindrical molds of 8 mm diameter and 4 mm height with only one open side to allow contact with the release medium and were then kept for 1 h in 100 % relative humidity to allow them to have sufficient cohesion. Two controls were prepared: a 0D-CPF and a control CPC which was prepared using the same composition and protocol as 2D-CPF but removing the foaming step. A Dissolution Tester (Pharma Alliance, USA) was used to evaluate the release following an adaptation of the USP Pharmacopeia Paddle Dissolution Test. Each sample was put in an individual amber glass filled with 150 mL of Phosphate Buffer Saline (PBS). Stirring conditions were set to 150 rpm and temperature to 37 ºC according to the current United States Pharmacopeia (USP) chapter <711> Dissolution [26]. Sampling consisted of the extraction of 1 mL aliquot and its replacement by 1 mL of fresh PBS at determined times up to 100 h. Four replicates of each kind of sample were evaluated.

Doxy was quantified by UV-VIS spectrophotometry using a microplate reader (Infinite M200 Pro Microplate Reader, TECAN, Switzerland), at the maximum wavelength of Doxy λ = 351 nm. This measurement was then corrected for evaporation,

sampling effect and degradation of the antibiotic as in previous studies [8] using MatLab software (The Mathworks Inc., USA). The percentage released was plotted as a function of time. Modeling was performed using the Korsmeyer Peppas (KP) model. The variable fitted is the quantity released M_t, normalised by the maximum quantity released M_∞ (Eq. 1).

$$M_t/M_\infty = k.t^n \qquad \text{Equation 1}$$

where k is a constant that accounts for structural parameters of the material and characteristics of the active principle such as the effective coefficient of diffusion. The exponent n allows the identification of the mechanism controlling the release. Specifically, for a given geometry of the sample it allows discerning between a release controlled by Fickian diffusion, swelling/case II transport or an intermediate situation. The KP model is applicable only up to 60 % of the quantity released. None of the CPFs reached that value after 100 h. Thus, the fitting was performed considering that M_∞ is unknown and that only the constant k is affected by the normalisation by M_∞. The exponent n describes the shape of the curve and is not affected by the normalisation. The quantity released as a function of time was thus fitted with the KP equation and both the value of the exponent n and the correlation coefficient R^2 were reported.

2.5. Antibacterial activity

The antibacterial activity of the materials was tested against two bacterial strains commonly found in osteoarticular as well as in nosocomial infections: *Staphylococcus Aureus* (*S.Aureus*) and *Escherichia Coli* (*E.Coli*) from the Culture Collection of the University of Göteborg, Sweden. The culture media was prepared by dissolving 3.7 wt% of Brain Heart Infusion broth (BHI, Scharlau, Spain) in distilled water, which was sterilised by autoclaving. To determine the antibacterial activity of the materials, the

agar diffusion test was used. This test allows determining the effectiveness of a diffusible anti-microbial agent, in our case an antibiotic, to inhibit the bacterial growth. The test was performed by plating 10^7 colony forming units (CFU) on agar plates, previously prepared with the appropriate culture media containing 1.5 % bacteriological agar (Scharlau, Spain). Three equidistant holes of 9.5 mm in diameter by 3 mm depth with a total volume of 0.23 cm^3 were performed in each agar plate. The freshly prepared CPFs were then injected in the hole taking special care to ensure lateral contact with the agar media. After incubation at 37 ºC overnight, the diameter of inhibition for each sample was measured using images of the plates taken with a digital camera. The inhibition zone was calculated from the diameter of the inhibition zone ($Ø_{iz}$) and the diameter of the material ($Ø_m$), according to Eq. 2 [27]. Three replicates of each formulation were used (n = 3).

$$Inhibition\ zone\ size = (Ø_{iz} - Ø_m)/2 \qquad \text{Equation 2}$$

2.6. *Statistics*

Statistical differences were determined using one-way ANOVA with Tukey's post-hoc tests using Minitab 16 software (Minitab, Inc., USA). Statistical significance was considered when $p < 0.05$. Data are presented as mean ± standard deviation.

3. Results

3.1. Material characterisation

To evaluate the potential influence of Doxy on the preparation process and on the properties of the CPFs, the effect of antibiotic addition on the surface tension of the liquid phase was measured. Various solutions were prepared containing 1 wt% of Tween 80 and different concentrations of Doxy. The surface tension of pure water,

72.37 ± 0.02 mN/m and Tween 80 (1 wt%), 39.66 ± 0.34 mN/m was also recorded as control (Fig. 2). Although increasing Doxy concentrations significantly decreased surface tension with a total difference of 8 % from 25 to 100 mg/mL solutions, the differences were small compared to the large reduction induced by the surfactant.

The plastic limit of non-foamed CPCs, defined as "the minimum amount of liquid that had to be added to a powder to form a paste" [23] was evaluated as a function of the amount of Doxy added to the solid phase (Fig. 3), as an indication of the ease of producing a paste at different Doxy concentrations. No statistically significant differences ($p > 0.05$) were observed between the plastic limit of pastes with no or low quantities of Doxy i.e. from 0D-CPF to 2D-CPF. However, the plastic limit increased significantly for 3D-CPF and 4D-CPF, $p=0.03$ and 0.05 respectively, so these formulations required more water to form a paste. Also, at constant liquid-to-powder ratio a system containing more Doxy appeared "drier" than a mixture containing less Doxy.

All Doxy-containing formulations presented excellent cohesion i.e. level 4. Even injecting the paste readily after preparation, the foams kept the integrity, and were intact after 24 h immersion in water, without any particle released to the surrounding medium. Only in the 0D-CPF a small fraction of particles detached from the paste, although the foam did not disintegrate, and the paste was able to consolidate after 24 h, thus recorded as level 3.

Figure 4 shows the injectability as well as the injection force required to extrude the CPF pastes. It can be observed that all Doxy-containing foams were injectable i.e. more than 80 % of the foamed paste could be extruded, with relatively low injection force values, between 25 and 30 N.

Calcium deficient hydroxyapatite (CDHA) was obtained as a result of the hydrolysis of α-TCP in all CPFs, in agreement with previous studies [4, 11]. The addition of Doxy resulted in a slight increase of unreacted α-TCP, from around 1 % for 0-CPF to 4-7 % for 1,2,3 and 4D-CPF, but no clear dose-dependency was observed (Supplementary information, Fig. S1). The SSA of CPFs increased from 20 to 30 m^2/g with increasing amounts of Doxy (Table 2), until a plateau value of approximately 31 m^2/g for loadings above 1.77 wt%, corresponding to 2D-CPF.

The morphology of the foams obtained with different amounts of Doxy is shown in Fig. 5. The macrostructure of the CPFs was clearly dependent on the amount of Doxy loaded. At higher Doxy concentrations, the foam-like structure of the materials was damaged and led to its collapse in some areas, which appeared less porous in the case of the 3D-CPFs and 4D-CPFs.

More detailed SEM images of the fracture surfaces of the 0D-CPF and 2D-CPF samples are shown in Fig. 6, both at low and high magnifications. Macropores were spherical and interconnections between adjacent pores were observed in the walls of most of them. Imaging of the pore walls revealed that 0D-CPF presented separate spherical aggregates of needle-like crystals resulting from the dissolution of individual α-TCP particles and precipitation of calcium-deficient hydroxyapatite crystals. The 2D-CPF showed the same basic structure of crystalline aggregates but with the particularity that on the pore walls the entangled matrix of plate-like crystals had grown flat possibly due to combined presence of Doxy and Tween at the interface with air.

The skeletal density of non-foamed CPCs determined by helium pycnometry was not affected by the addition Doxy and was 2.75 ± 0.02 $g.cm^{-3}$. The total porosity and total macroporosity of the different CPFs measured by mercury immersion, together

with the interconnected porosity and interconnected macroporosity recorded by MIP are shown in Fig. 7a. The pore entrance size distribution (PESD) in the foams containing different amounts of antibiotic is displayed in Fig. 7b. Total porosity showed minor variations, from 71.98 ± 4.94 % in 0D-CPF to 65.99 ± 7.39 % in 4D-CPF. The addition of antibiotic to the CPFs led to a gradual reduction of the total macroporosity from 50.2 ± 4.9 % for an antibiotic-free 0D-CPF to 22.8 ± 7.4 % for a 4D-CPF. Focusing on the doxy-containing CPFs, the total macroporosity decreased linearly with increasing amount of Doxy at a rate of approximately 10 % every 25 mg of Doxy. Moreover, more than 2/3 of the total macroporosity was interconnected except for 4D-CPF, where the percentage of interconnected macropores was lower.

The PESD was bimodal in all formulations containing Doxy, with the peaks centred around 50 nm and 100 μm, while the 0D-CPF showed an additional peak in the micrometer range, at 3 μm. The diameter of open macropores i.e. those greater than 10 μm as previously defined, slightly decreased with increasing amount of antibiotic. The intensity and position of the peak centred at 50 nm of all antibiotic-containing CPFs slightly increased with increasing amount of Doxy, while the pristine CPF showed bigger pore entries with a mode diameter around 100 nm. The images obtained by micro-computed tomography for 0D-CPF and 2D-CPF shown in Fig. 8 provide an outlook of the morphology and macrostructure of these materials. The 2D-CPF showed smaller and less-defined macropores compared to the 0D-CPF.

3.2. Antibiotic release profile

The Doxy release kinetics was evaluated for all CPF formulations. The percentage released is represented as a function of time (Fig. 9a) for all CPFs and for a 2D-CPC, the non-foamed counterpart of the 2D-CPF. The initial quantity loaded, the

final quantity released and the corresponding percentage released after 5 days are reported in Fig. 9b, while the relationship between final percentage released and interconnected macroporosity is represented in Fig. 9c. CPFs released a decreasing drug percentage with increasing initial amount of Doxy (Fig. 9 a and b), from 54.88 ± 5.82 % to 19.58 ± 2.59 % from 1D-CPF to 4D-CPF, respectively. In none of the cases was a burst release observed; instead, the rate of release slowly decreased with time (Fig. 9a). The different formulations displayed potential for longer release, as the stationary state was not reached in the timeframe of this study. A maximum of 1 mg was released by 2D-CPFs in 5 days. The percentage released was found to be proportional to the macroporosity of the CPF (Fig. 9c), fitting linearly with a slope of 1.23 which suggested that interconnected macroporosity had a major influence on the percentage released. The KP model was applied to interpret the release kinetics of the CPFs. The fitting parameters are reported in Table 3.

3.3. Antibacterial activity

The antibacterial activity of the materials against *S. Aureus* and *E. Coli* is shown in Fig. 10a. All antibiotic-containing materials displayed antibacterial properties, while the pristine, 0D-CPF used as control showed no bacterial inhibition. Concerning *E. Coli*, the 2D-CPC, 1D-CPF and 2D-CPF presented similar inhibition zone sizes. The 3D-CPF and 4D-CPF showed a higher value ($p < 0.05$). The diffusion test with the *S. Aureus* strain did not reveal statistically significant differences between materials. When comparing the CPFs with their non-foamed counterpart 2D-CPC, no differences in the inhibition zone size were recorded. To further understand this result, the Doxy loading and the apparent density as determined by MIP of each material were used to calculate the absolute amount of antibiotic in the agar hole at the beginning of the test, reported in Table 4.

The absolute amount of Doxy present in the material at the beginning of the test was used to normalise the inhibition zone size (Fig. 10b). After normalisation, it was clear that macroporous matrices were more efficient than dense matrices regardless of the amount of active principle loaded. The bacteriostatic effect of the materials tested decreased with macroporosity.

4. Discussion

The CPFs developed in this work combine a number of major advantages as bone grafting materials able to locally deliver antibiotic. Together with the injectability, self-setting ability, and intrinsic nano/microporosity characteristic of CPCs, they exhibit a significant interconnected macroporosity that is known to be crucial for cell colonisation, angiogenesis and, in general, for the events leading to bone regeneration [7, 11, 28]. In this work we demonstrated that the interconnected macroporosity of the injectable CPFs designed had also a significant impact in the control of the drug release kinetics of Doxycycline hyclate.

To generate the macroporous structures, a 1 wt% Tween80 solution was used as foaming agent. Since the surface tension changes produced by antibiotic on this solution were minor (Fig. 2), they were not expected to significantly affect foamability. In contrast, a clear effect on the plastic limit was registered upon the addition of high concentrations of Doxy (Fig. 3), suggesting that Doxy absorbed water, resulting in a drying effect on the unfoamed paste. An increased shear stress was thus needed to mix the powder phase with the foamed liquid phase, which can explain the partial collapse of the foamed template at high contents of Doxy, as observed in the optical microscope images (Fig. 5) and corroborated by the macroporosity results (Fig. 7a). Anyhow, this

was not detrimental to their injectability which was maintained in all formulations, and is an essential requirement to ensure their clinical applicability.

The general outlook to the material macrostructure obtained by micro computed tomography reconstructions (Fig. 8) confirmed that the addition of Doxy reduced both the size of the macropores and the number of their interconnections.

The addition of Doxy did not prevent the foam's setting reaction (Supplementary material Fig. S1), where the dissolution of α-TCP was followed by the precipitation of CDHA [4, 11]:

$$Ca_3(PO_4)_{2\,(s)} + H_2O_{(l)} \rightarrow Ca_9(HPO_4)(PO_4)(OH)_{(s)}$$

However, the presence of the antibiotic was related to an increase of SSA (Table 2) which was associated to its effect on the microstructure of the CDHA crystals formed. In fact, it was suggested in a previous study [8] that, due to its Ca-chelating ability, Doxy can act in this kind of systems as a nucleating agent, promoting the formation of smaller crystals and leading to a more homogeneous microstructure, as shown in Fig. 6. This is in agreement also with the disappearance -in the MIP diagram of the Doxy-containing samples (Fig. 7b) of the peak around 3-5 μm detected in the pristine foams.

The introduction of macroporosity in the CPCs clearly modified the drug release profile, as observed when comparing the 2D-CPF with its non-foamed counterpart 2D-CPC. The percentage released from CPFs was significantly higher in all cases compared to the 2D-CPC (Fig. 9b). However, the interdependence between Doxy concentration and macroporosity introduced additional complexity in the system. The addition of Doxy led to a progressive loss of total porosity as well as of interconnected macroporosity (Fig. 7a) and a reduction in the entrance pore size of the macropores

(Fig. 7b). This was shown to be highly relevant for their drug release properties; Different release kinetics were observed in the CPFs depending on the amount of Doxy loaded; the rate of percentage released decreased with increasing Doxy concentrations, which can be related to the lower volume of macropores and their smaller size (Fig. 8 and 7b). Although CPFs were more porous than CPCs, and thus a lower amount of Doxy was present in the same volume, CPFs released a higher absolute amount of Doxy after 5 days, with a maximum of 1 mg for the 2D-CPF.

Besides, the uniform distribution of the drug in the matrix of all formulations studied was revealed by the progressive release observed i.e. no initial burst (Fig. 9a). In general, the availability of active principles to the bone is limited and slow, as compared to soft tissues or other organs for instance. The on site direct bioavailability of the active principle, in our case Doxycycline hyclate, maximized the efficiency of the treatment. The extended drug release profiles obtained with the present CPFs are highly desirable in controlled drug delivery matrices, as a reproducible rate and prolonged delivery are obtained, and allow lower amount of drugs to be used [29].

For the treatment of infection, ideally a high concentration of antibiotics is needed in the first 1–2 days and thereafter a prolonged release of a lower concentration should be maintained for another 4 weeks [30]. Although the lack of burst release may be a disadvantage when dealing with prophylactic therapy of infections, the CPFs designed here can be envisaged in this case as a complementary therapy to an initial parenteral or oral antibiotic administration, delivering Doxy on-site for the continuation of the treatment, and thus improving patient compliance. For instance, the 3D-CPF and 4D-CPF showed potential for release during 3 or 4 weeks, suitable for bone infection treatment.

The close relationship between different structural properties such as SSA, macroporosity, interconnected macroporosity, porosity and interconnected porosity was put forward by their direct correlation with the percentage released by the CPFs using a linear fit (not shown). The quality of fit obtained, estimated through the correlation coefficient (R^2), was 0.842, 0.957, 0.918, 0.931 and 0.910 for SSA, macroporosity, interconnected macroporosity, porosity and interconnected porosity, respectively. The good correlation between the amount of macroporosity and the percentage of Doxy released (Fig. 9c) confirmed that macroporosity plays a key role in the drug release phenomena by enhancing fluid exchange and increasing the accessible surface, thus facilitating drug delivery and availability.

The fitting of the release profiles led to n values comprised between 0.50 and 1.00 (Table 3), which for a planar geometry corresponds to a non-Fickian diffusional release [31, 32]. It is known that a non-Fickian transport may be due to structural changes, temperature, saturation of the release media, etc. As the experiments were performed in sink conditions, and following standards [26], this non-Fickian behavior could be attributed to the self-setting nature of CPFs. Their microstructure evolving over time is responsible for the anomalous diffusion, as shown in previous works [8].

All antibiotic-containing CPFs showed bacteriostatic effect on both *E. Coli* and *S. Aureus* (Fig. 10a) in an agar diffusion test. *E. Coli* was selected as the most commonly found bacteria in nosocomial infections together with *S. Aureus*, which is also very often responsible of osteo-articular infections. The results obtained were function of both the matrix ability to release the active principle and the initial amount of active principle present in the material. In this kind of test where solid-solid contact i.e. agar – material, is crucial for the diffusion of the antibiotic, the architecture of the material plays an important role: while the unfoamed CPC has an optimum contact with

the agar, the macroporosity of the CPF revert in few contact points with the agar, hampering the diffusion of the material. Additionally, no direct correlation can be sought between the release in liquid media in sink conditions with free diffusivity and the release established in agar. Nevertheless, this test has shown the antibacterial efficiency of the material.

As the same volume of material was placed in the agar, for the same wt% of Doxy in the material the absolute quantity of antibiotic present is lower when the matrix used is more porous. The inhibition zone size was thus normalised by the absolute quantity of Doxy present in the material. The results proved that, even in the static conditions of this test and the lower amount of contact points with the agar, the interconnected macroporous structure exhibited by the CPFs was more efficient in terms of ensuring antibiotic availability than their microporous counterpart, namely CPCs (Fig. 10b, Table 4).

Different antibiotic release profiles are reported in the literature for calcium phosphate cements: from slow releasing dosage forms [8, 33–36] to very fast burst release of the antibiotic [37, 38]. Although some approaches successfully prevented the risk of antibiotic resistance by releasing almost all the drug loaded [39], the dosage forms did not present an adequate macrostructure to enhance bone ingrowth. The calcium phosphate foams presented in this study exhibit a progressive release profile up to 1 mg in 5 days, corresponding to 55% of the quantity loaded in 2D-CPC, with potential for complete release and a simultaneous interconnected macroporosity of around 25 % (Fig. 9c) that is expected to enhance, in addition, tissue colonisation.

It has been put forward that tetracyclines inhibit bone resorption through different mechanisms such as decreased osteoclast activity, so incomplete release of the drug

could be detrimental [40]. In the case of CPCs, it has been commonly observed that 100 % release is not reached, regardless of the active principle used [6]. This aspect, which can be very significant in the case of CPCs, is expected to be minimized thanks to the macroporous structure of the foams. In fact, it has been shown that the presence of an interconnected network of macropores in the material enhances its resorption rate [41]. Thus, in case there was some unreleased residual Doxy in the material, the low quantities employed in the loading of the CPFs, and their macroporosity enhancing fluid circulation and resorption rate would minimize the inhibiting effects of Doxy on osteoclasts, in addition to potential bacterial resistance.

5. Conclusion

Calcium Phosphate Foams (CPFs) were shown to be attractive drug delivery systems for osteo-articular applications as compared to Calcium Phosphate Cements (CPCs), since they overcome several of their limitations. First, CPFs exhibited an interconnected macroporous structure while maintaining injectability, cohesion and self-setting ability, thus providing a template for bone ingrowth. Second, CPFs were more efficient as drug release systems, since less active principle was loaded and higher percentages and absolute amounts were released after 5 days, with potential for longer release. The therapeutic effect is expected to increase, while the risk of generating antibiotic-resistant bacteria due to the antibiotic still present in the matrix is reduced. Finally, the control of both macrostructure and release profile allowed designing versatile and efficient drug delivery systems that can be adapted to different applications. While CPFs are limited to non-load bearing applications, the combination of a prophylactic antibiotic release with a biomimetic composition and structure makes

them an attractive solution to today's challenges in the fields of orthopaedics, spine and maxillofacial bone regeneration.

Acknowledgements

Authors acknowledge the Spanish Government for financial support through Project MAT2012-38438-C03-01, co-funded by the EU through European Regional Development Funds, and Ramon y Cajal fellowship of CC. Support for the research of MPG was received through the prize "ICREA Academia" for excellence in research, funded by the Generalitat de Catalunya. Authors thank Dr. A. Navarro for kindly allowing access to his lab for surface tension determinations. Authors also acknowledge Dr. S. Meille and Prof. J. Chevalier for giving us access to µCT instrument at the UMR CNRS 5510 (MATEIS), Insa Lyon.

6. References

[1] Dorozhkin S V. Calcium orthophosphate cements for biomedical application. J Mater Sci 2008;43:3028–57.

[2] Ginebra M-P, Traykova T, Planell JA. Calcium phosphate cements as bone drug delivery systems: a review. J Control Release 2006;113:102–10.

[3] Ginebra M-P, Traykova T, Planell JA. Calcium phosphate cements: competitive drug carriers for the musculoskeletal system? Biomaterials 2006;27:2171–7.

[4] Espanol M, Perez RA, Montufar EB, Marichal C, Sacco A, Ginebra M-P. Intrinsic porosity of calcium phosphate cements and its significance for drug delivery and tissue engineering applications. Acta Biomater 2009;5:2752–62.

[5] Verron E, Khairoun I, Guicheux J, Bouler J-M. Calcium phosphate biomaterials as bone drug delivery systems: a review. Drug Discov Today 2010;15:547–52.

[6] Ginebra M-P, Canal C, Espanol M, Pastorino D, Montufar EB. Calcium phosphate cements as drug delivery materials. Adv Drug Deliv Rev 2012;64:1090–110.

[7] Otsuki B, Takemoto M, Fujibayashi S, Neo M, Kokubo T, Nakamura T. Pore throat size and connectivity determine bone and tissue ingrowth into porous implants: three-dimensional micro-CT based structural analyses of porous bioactive titanium implants. Biomaterials 2006;27:5892–900.

[8] Canal C, Pastorino D, Mestres G, Schuler P, Ginebra M-P. Relevance of microstructure for the early antibiotic release of fresh and pre-set calcium phosphate cements. Acta Biomater 2013;9:8403–12.

[9] Tsourvakas S. Local Antibiotic Therapy in the Treatment of Bone and Soft Tissue Infections. In: Danilla S, editor. Selected Topics in Plastic Reconstructive Surgery. InTech, open access; 2012. p17-44.

[10] Habraken WJEM, Wolke JGC, Jansen J a. Ceramic composites as matrices and scaffolds for drug delivery in tissue engineering. Adv Drug Deliv Rev 2007;59:234–48.

[11] Montufar EB, Traykova T, Gil C, Harr I, Almirall A, Aguirre A, et al. Foamed surfactant solution as a template for self-setting injectable hydroxyapatite scaffolds for bone regeneration. Acta Biomater 2010;6:876–85.

[12] Montufar EB, Traykova T, Planell JA, Ginebra M-P. Comparison of a low molecular weight and a macromolecular surfactant as foaming agents for injectable self setting hydroxyapatite foams: Polysorbate 80 versus gelatine. Mater Sci Eng C 2011;31:1498–504.

[13] Ginebra M-P, Delgado J-A, Harr I, Almirall A, Del Valle S, Planell JA. Factors affecting the structure and properties of an injectable self-setting calcium phosphate foam. J Biomed Mater Res A 2007;80:351–61.

[14] Saint-Jalmes A, Peugeot M-L, Ferraz H, Langevin D. Differences between protein and surfactant foams: Microscopic properties, stability and coarsening. Colloids Surfaces A Physicochem Eng Asp 2005;263:219–25.

[15] Pountos I, Georgouli T, Bird H, Kontakis G, Giannoudis P V. The effect of antibiotics on bone healing: current evidence. Expert Opin Drug Saf 2011;10:935–45.

[16] Kallala R, Graham SM, Nikkhah D, Kyrkos M, Heliotis M, Mantalaris A, et al. *In vitro* and *in vivo* effects of antibiotics on bone cell metabolism and fracture healing. Expert Opin Drug Saf 2012;11:15–32.

[17] Ong SM, Taylor GJS. Doxycycline inhibits bone resorption by human interface membrane cells from aseptically loose hip replacements. J Bone Joint Surg Br 2003;85:456–61.

[18] Preshaw PM, Hefti AF, Jepsen S, Etienne D, Walker C, Bradshaw MH. Subantimicrobial dose doxycycline as adjunctive treatment for periodontitis. A review. J Clin Periodontol 2004;31:697–707.

[19] Job-Deslandre C, Krebs S, Kahan A. Chronic recurrent multifocal osteomyelitis: five-year outcomes in 14 pediatric cases. Joint Bone Spine 2001;68:245–51.

[20] Roeder B, Van Gils CC, Maling S. Antibiotic beads in the treatment of diabetic pedal osteomyelitis. J Foot Ankle Surg 2000;39:124–30.

[21] Bartkowski SB, Zapala J, Heczko P, Szuta M. Actinomycotic osteomyelitis of the mandible: review of 15 cases. J Cranio-Maxillo-Facial Surg 1998;26:63–7.

[22] Thompson S, Townsend R. Pharmacological agents for soft tissue and bone infected with MRSA: which agent and for how long? Injury 2011;42 Suppl 5:S7–10.

[23] Bohner M, Baroud G. Injectability of calcium phosphate pastes. Biomaterials 2005;26:1553–63.

[24] Montufar EB, Maazouz Y, Ginebra MP. Relevance of the setting reaction to the injectability of tricalcium phosphate pastes. Acta Biomater 2013;9:6188–98.

[25] Almirall A, Larrecq G, Delgado J. Fabrication of low temperature macroporous hydroxyapatite scaffolds by foaming and hydrolysis of an α-TCP paste. Biomaterials 2004;25:3671–80.

[26] United States Pharmacopeia and National Formulary, Dissolution <711>. Rockville, MD: US Pharmacopeial Convention; 2008:267-274.

[27] Bauer AW, Kirby WM, Sherris JC, Turck M. Antibiotic susceptibility testing by a standardized single disk method. Am J Clin Pathol 1966;45:493–6.

[28] Mastrogiacomo M, Scaglione S, Martinetti R, Dolcini L, Beltrame F, Cancedda R, et al. Role of scaffold internal structure on *in vivo* bone formation in macroporous calcium phosphate bioceramics. Biomaterials 2006;27:3230–7.

[29] Ding X, Alani A, Robinson J. Remington. The Science and Practice of Pharmacy. In: Hendrickson R, editor. Remington Science and Practice of Pharmacy. Groningen: Lippincott Williams & Wilkins; 2006. p 939–964.

[30] Geurts J, Chris Arts JJ, Walenkamp GHIM. Bone graft substitutes in active or suspected infection. Contra-indicated or not? Injury 2011;42 Suppl 2:S82–6.

[31] Siepmann J, Peppas N a. Higuchi equation: derivation, applications, use and misuse. Int J Pharm 2011;418:6–12.

[32] Ritger PL, Peppas NA. A simple equation for description of solute release I. Fickian and non-fickian release from non-swellable devices in the form of slabs, spheres, cylinders or discs. J Control Release 1987;5:23–36.

[33] Liu W, Chang J. *In vitro* evaluation of gentamicin release from a bioactive tricalcium silicate bone cement. Mater Sci Eng C 2009;29:2486–92.

[34] Kisanuki O, Yajima H, Umeda T, Takakura Y. Experimental study of calcium phosphate cement impregnated with dideoxy-kanamycin B. J Orthop Sci 2007;12:281–8.

[35] Takechi M, Miyamoto Y, Ishikawa K, Nagayama M, Kon M, Asaoka K, et al. Effects of added antibiotics on the basic properties of anti-washout-type fast-setting calcium phosphate cement. J Biomed Mater Res 1998;39:308–16.

[36] Vorndran E, Geffers M, Ewald A, Lemm M, Nies B, Gbureck U. Ready-to-use injectable calcium phosphate bone cement paste as drug carrier. Acta Biomater 2013;9:9558–67.

[37] Alkhraisat MH, Rueda C, Cabrejos-Azama J, Lucas-Aparicio J, Mariño FT, Torres García-Denche J, et al. Loading and release of doxycycline hyclate from strontium-substituted calcium phosphate cement. Acta Biomater 2010;6:1522–8.

[38] David Chen C-H, Chen C-C, Shie M-Y, Huang C-H, Ding S-J. Controlled release of gentamicin from calcium phosphate/alginate bone cement. Mater Sci Eng C 2011;31:334–41.

[39] Schnieders J, Gbureck U, Vorndran E, Schossig M, Kissel T. The effect of porosity on drug release kinetics from vancomycin microsphere/calcium phosphate cement composites. J Biomed Mater Res B Appl Biomater 2011;99:391–8.

[40] Bettany JT, Peet NM, Wolowacz RG, Skerry TM, Grabowski PS. Tetracyclines induce apoptosis in osteoclasts. Bone 2000;27:75–80.

[41] Del Valle S, Mino N, Munoz F, Gonzalez A, Planell JA, Ginebra MP. *In vivo* evaluation of an injectable macroporous calcium phosphate cement. J Mater Sci Mater Med 2007;18:353-61.

Figure Captions

Figure 1: Structural formula of Doxycycline hyclate.

Figure 2: Surface tension measurements dissolutions of Tween (1 wt%) containing different amounts of Doxy (25, 50, 75 and 100 mg/mL) equivalent to the 1D-CPF, 2D-CPF, 3D-CPF and 4D-CPF respectively. Dashed lines indicate the surface tension of water and of a 1 %Tween 80 solution (0D-CPF). (n=10).

Figure 3: Plastic limit of non-foamed materials for different Doxy loadings. *, ** indicate statistically significant groups ($p<0.05$).

Figure 4: Injection force (N) and injectability (%) of pristine and antibiotic-loaded calcium phosphate foams. • and + represent statistically significant differences ($p<0.05$) between compositions with the same symbol.

Figure 5: Optical microscope images of the CPFs obtained with different concentrations of Doxy, from left to right: 0D-CPF, 1D-CPF, 2D-CPF, 3D-CPF and 4D-CPF.

Figure 6: FESEM images of the fracture surface of CPFs with detail of the macropore walls of a 0D-CPF (left) and a 2D-CPF (right) at different magnifications: 50x, 2500x and 10000x (from top to bottom).

Figure 7: Porosity characterisation of CPFs containing different amounts of Doxy: (a) Total porosity and total macroporosity as measured by immersion in Hg (n=12); interconnected porosity and interconnected macroporosity as determined by MIP (n=4); and (b) MIP pore entry size distribution (n=4).

Figure 8: 3D reconstruction of a micro-computed tomography scan of a 5x5x5 mm^3 cubic volume a 0D-CPF (a) and 2D-CPF (b)

Figure 9: (a) Release curves of CPFs containing different amounts of Doxy. A 2D-CPC is included for comparison; (b) Initial quantity loaded, final quantity released and final percentage released (100 h); (c) Final percentage released as a function of the macroporosity of the CPFs and CPC.

Figure 10: (a) Antibacterial activity against *Escherichia Coli* and *Staphylococcus Aureus* of CPFs containing different amounts of Doxy and a non-foamed 50-CPC counterpart. (b) Normalisation of the antibacterial activity by the absolute amount of antibiotic in the materials. For *E. Coli*, *, **, *** and **** indicate statistically significant differences ($p < 0.05$). For *S. Aureus*, •, ••, ••• and •••• indicate statistically significant differences ($p < 0.05$).

Tables

Table 1: Nomenclature of the different CPFs, amounts of water, calcium phosphate (CaP) powder and antibiotic, and corresponding weight percentage of antibiotic with respect to the total weight of the CPFs (Cdoxy).

Nomenclature	Liquid phase (mL)	CaP powder (g)	Doxy (mg)	Cdoxy (wt%)
0D-CPF	1	1.820	0	0
1D-CPF	1	1.820	25	0.88
2D-CPF	1	1.820	50	1.76
3D-CPF	1	1.820	75	2.64
4D-CPF	1	1.820	100	3.52

Table 2: Specific surface area (SSA, BET theory) of Doxy-containing CPFs.

Composition	SSA (m^2/g) ± SD
0D-CPF	20.25 ± 0.03
1D-CPF	23.47 ± 0.12
2D-CPF	30.47 ± 0.18
3D-CPF	31.77 ± 0.20
4D-CPF	30.94 ± 0.19

Table 3: Fitted parameters of the Korsmeyer Peppas model, type of limiting transport mechanism.

Formulation	n	R^2	Transport Mechanism
1D-CPF	0.63	0.9866	Non-fickian diffusion
2D-CPF	0.60	0.9982	Non-fickian diffusion
3D-CPF	0.57	0.9953	Non-fickian diffusion
4D-CPF	0.65	0.9961	Non-fickian diffusion

Table 4: Calculated parameters for antibiotic-loaded CPCs and CPFs employed in the antibacterial tests: concentration of Doxy, apparent density, and absolute amount of Doxy in the agar hole (0.23 cm^3).

Material	C_{doxy} (wt%)	Apparent density (g/cm^3)	Q_{doxy} (mg) in the agar defect
2D-CPC	1.76	1.290	5.22±0.69
1D-CPF	0.88	0.748	1.51±0.71
2D-CPF	1.76	0.808	3.27±0.67
3D-CPF	2.64	0.930	5.01±1.41
4D-CPF	3.52	0.932	7.55±2.44

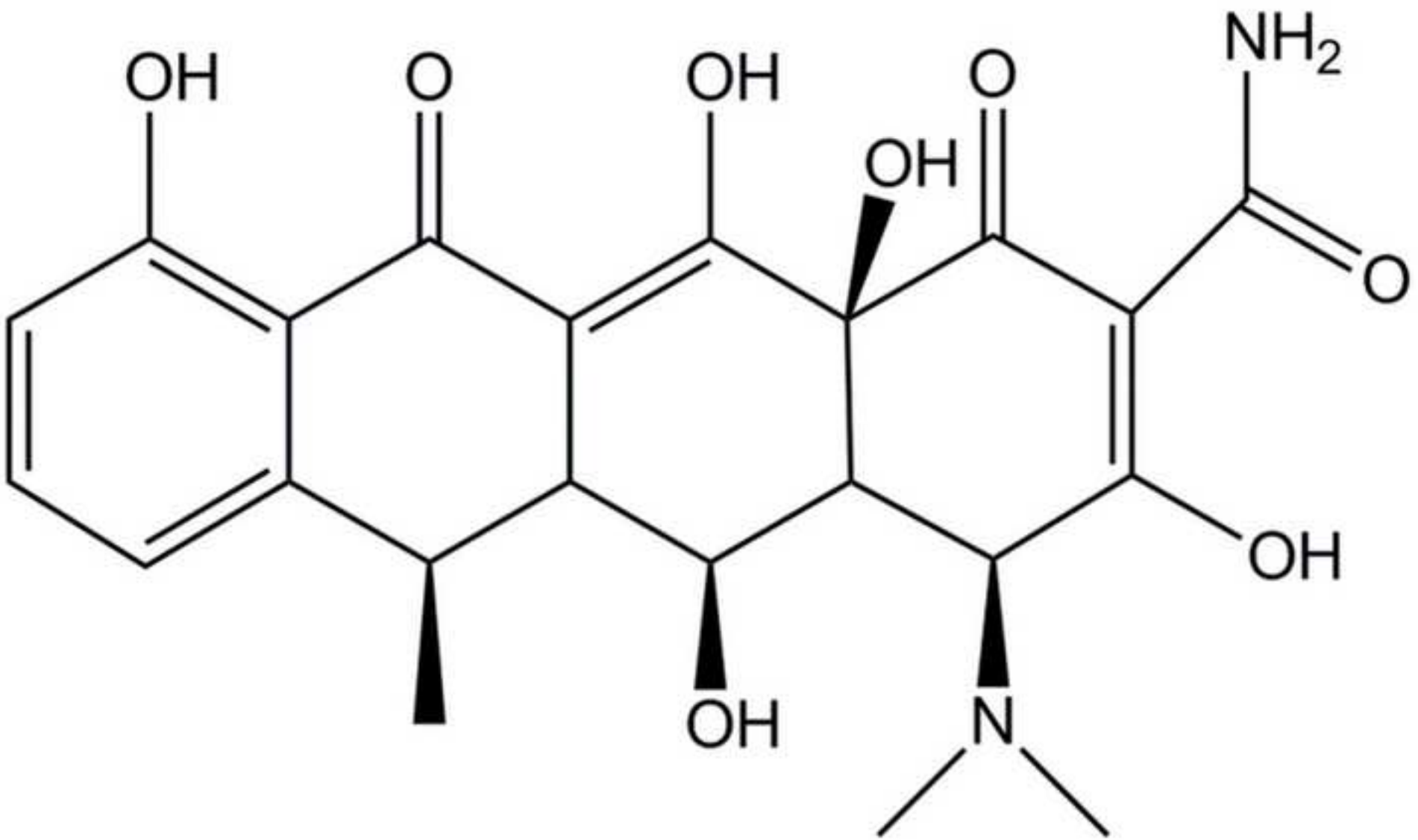

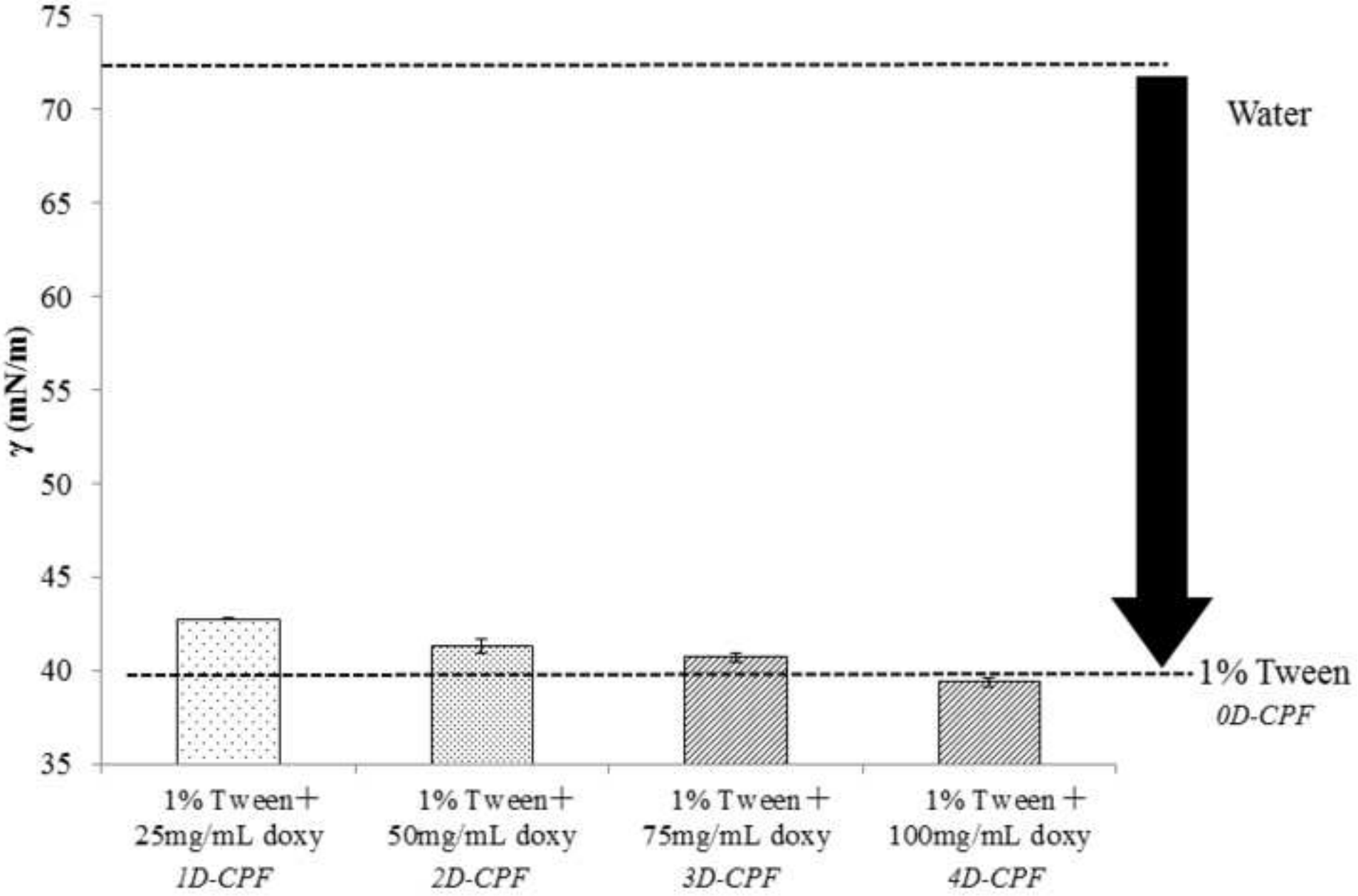

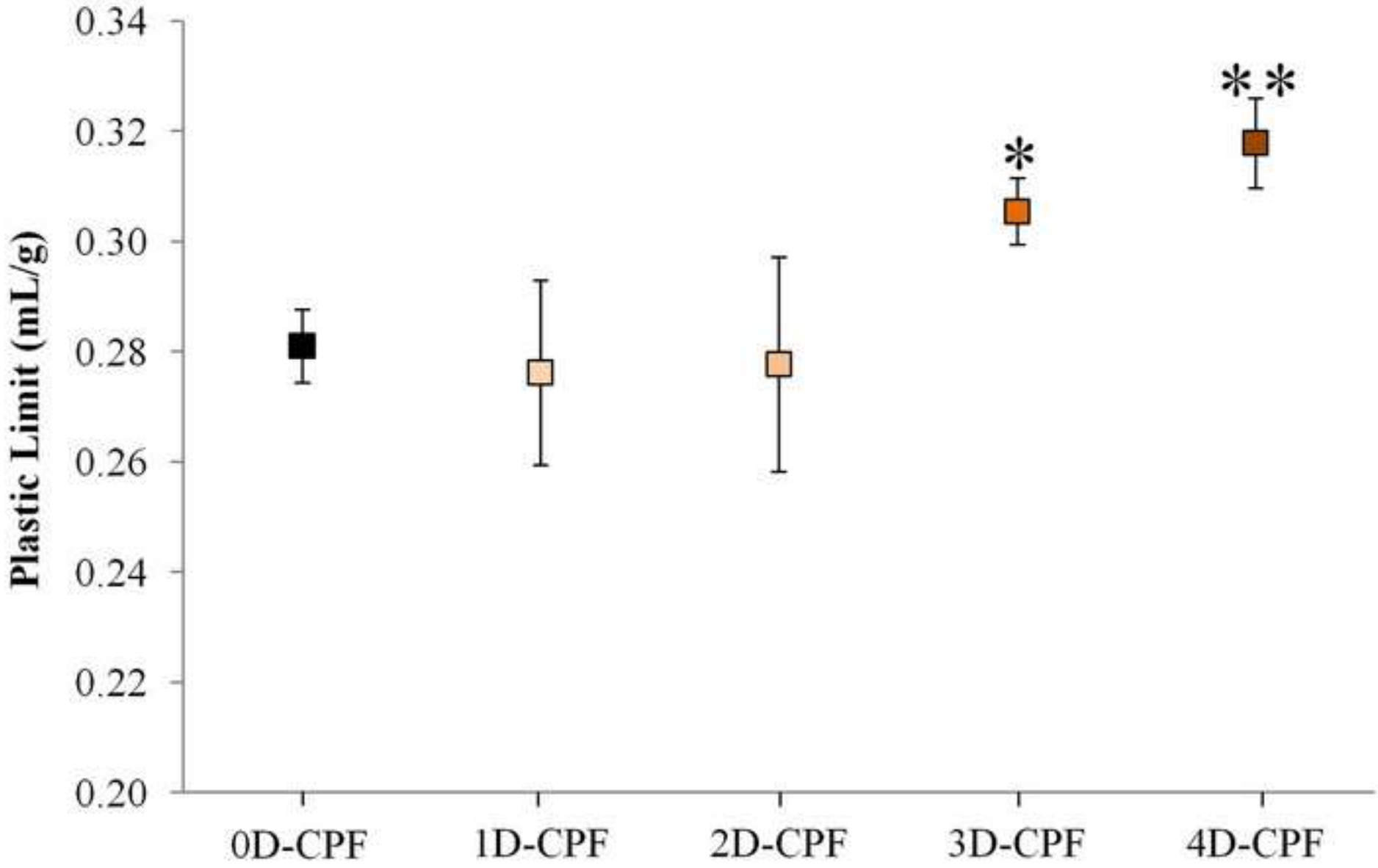

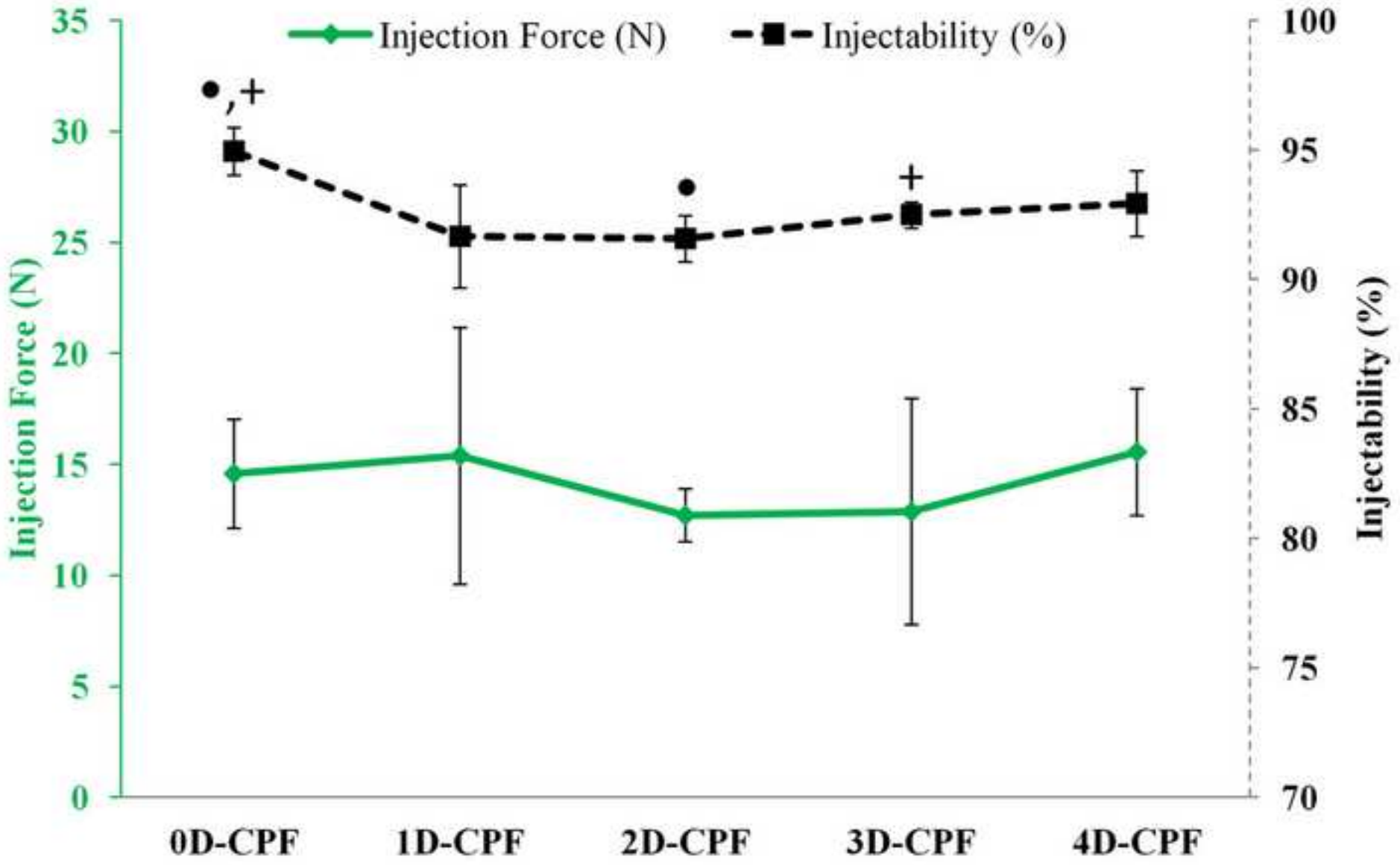

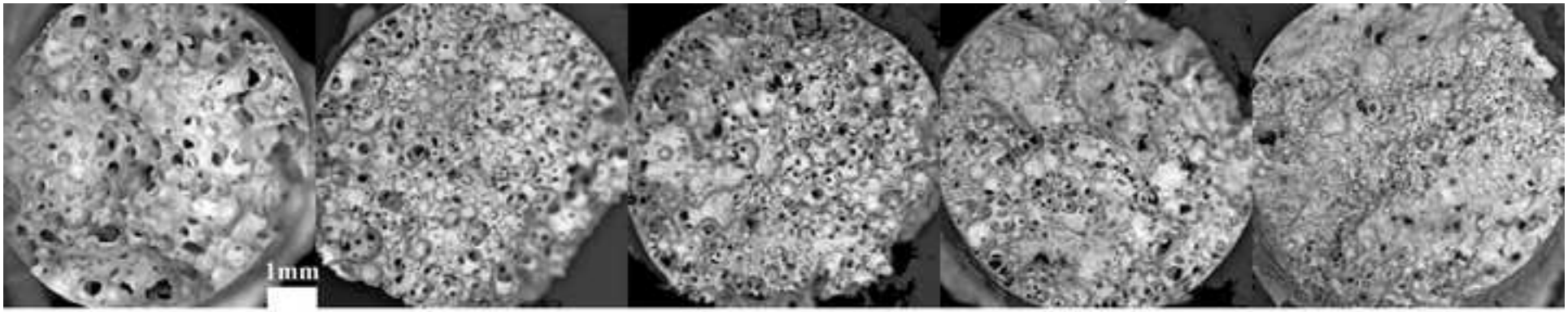

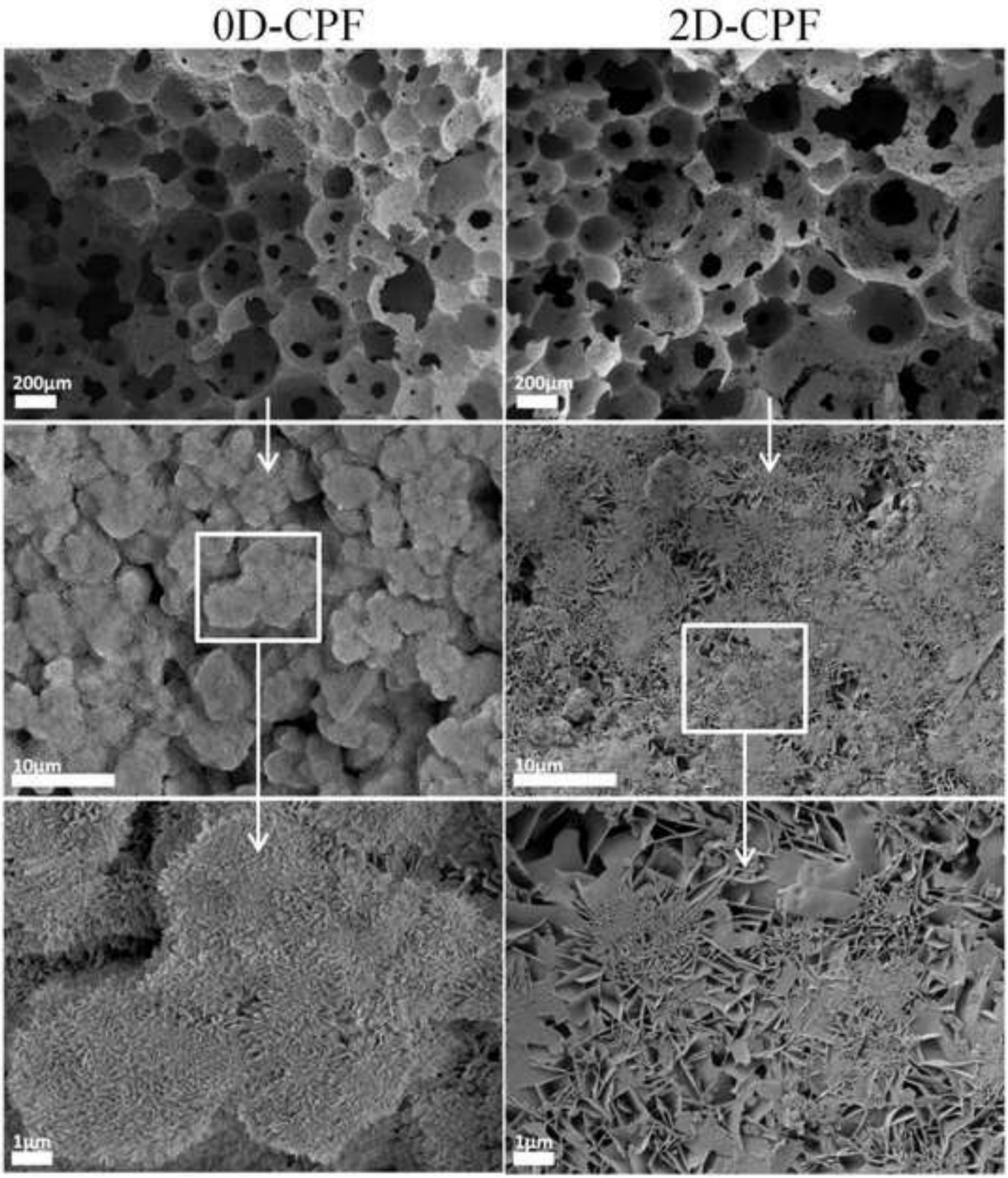

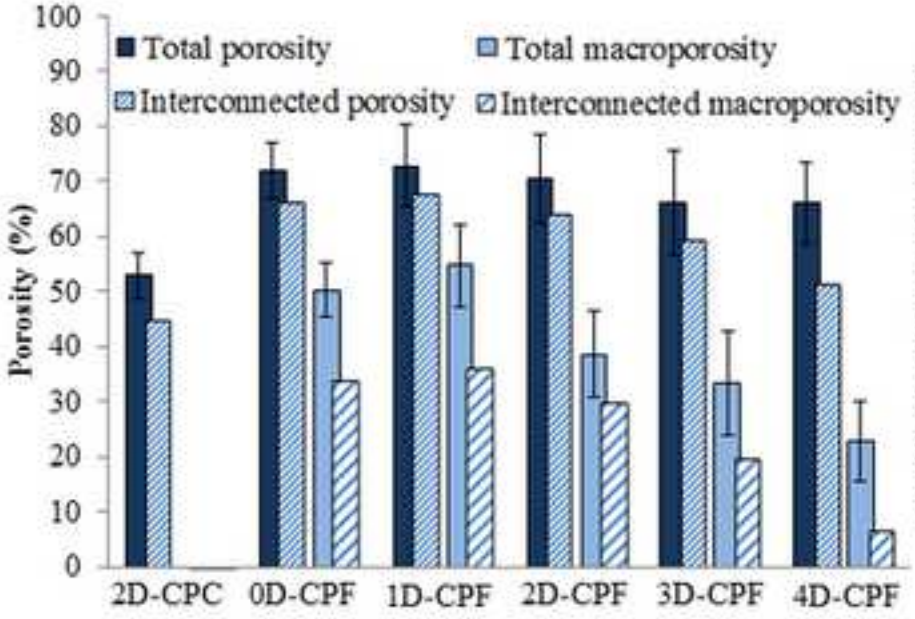

a)

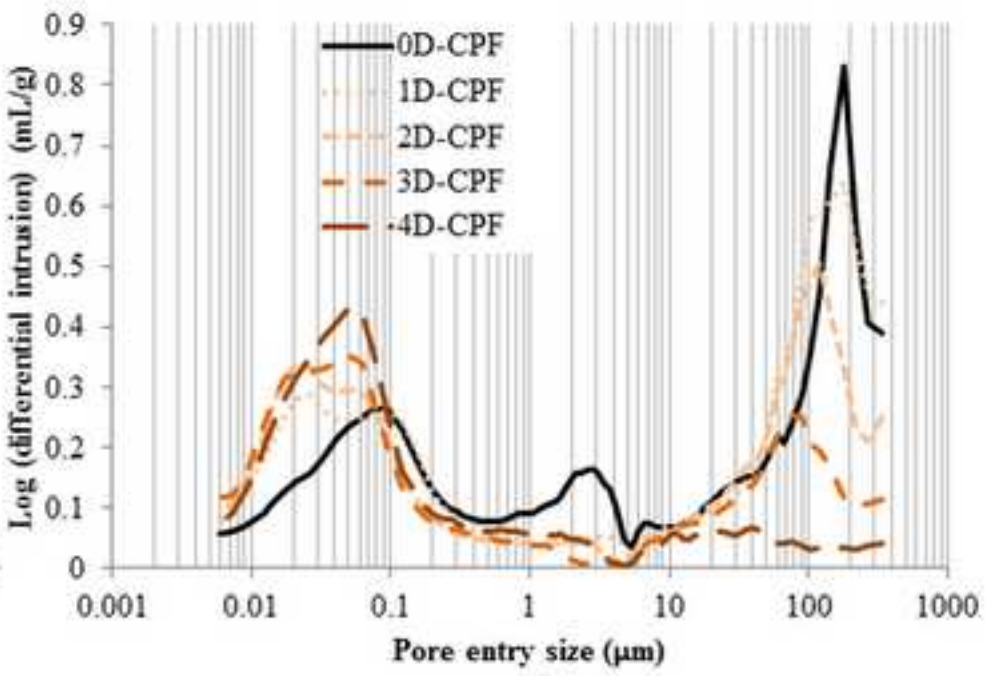

b)

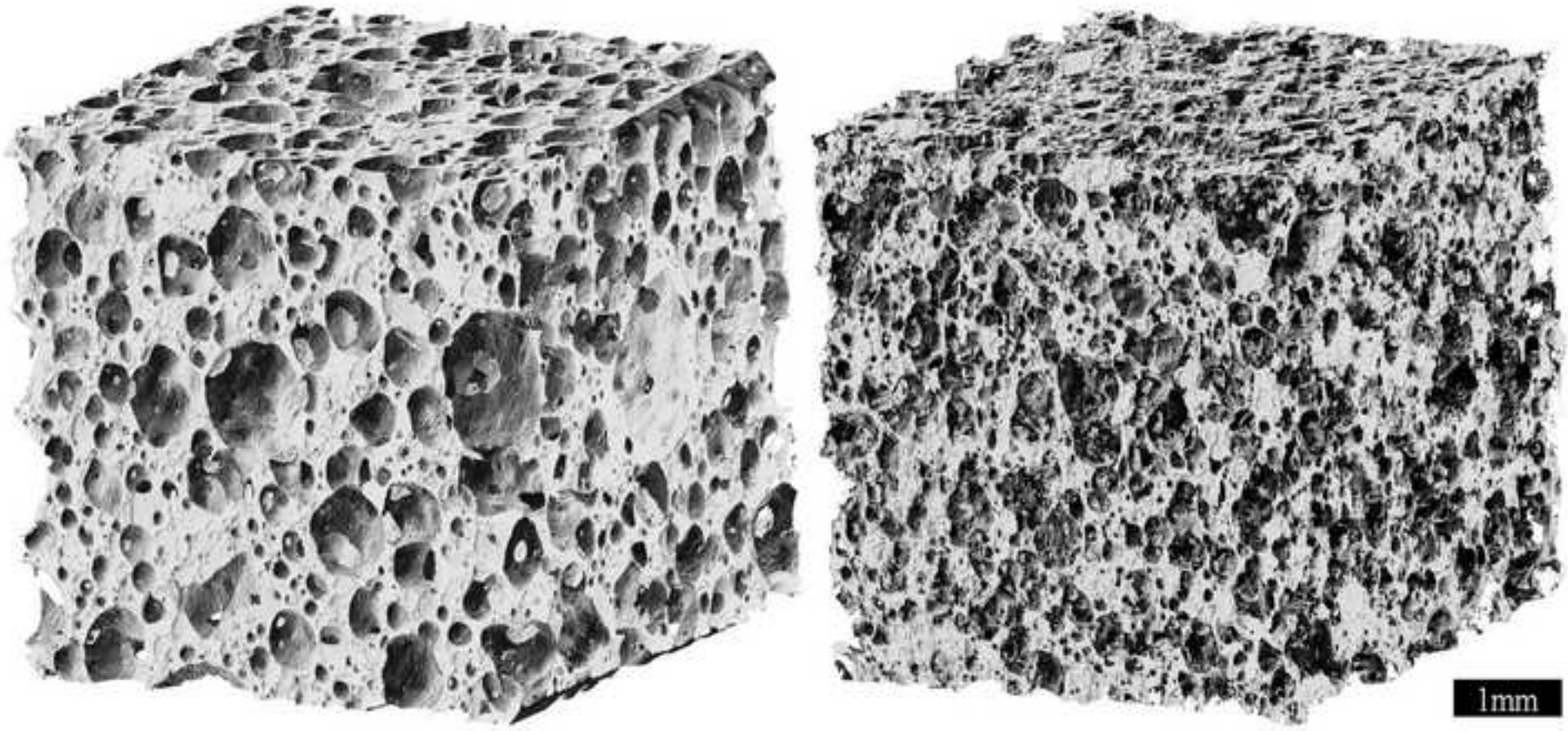

a) b)

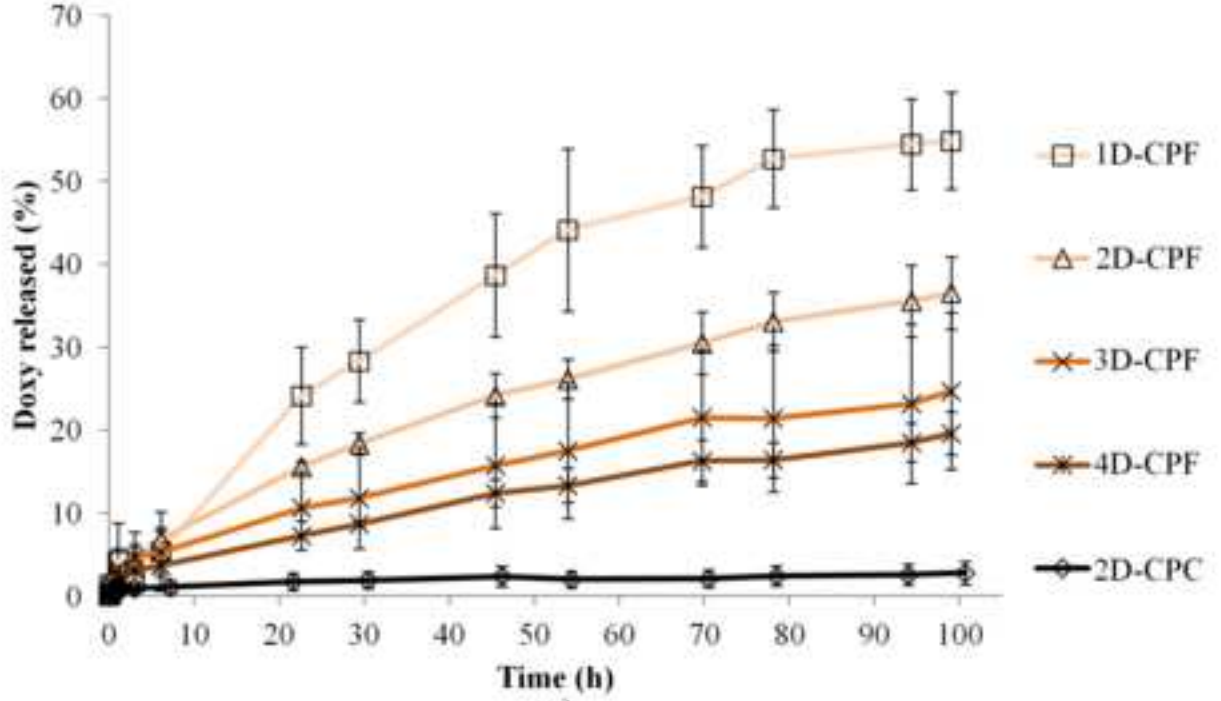

a)

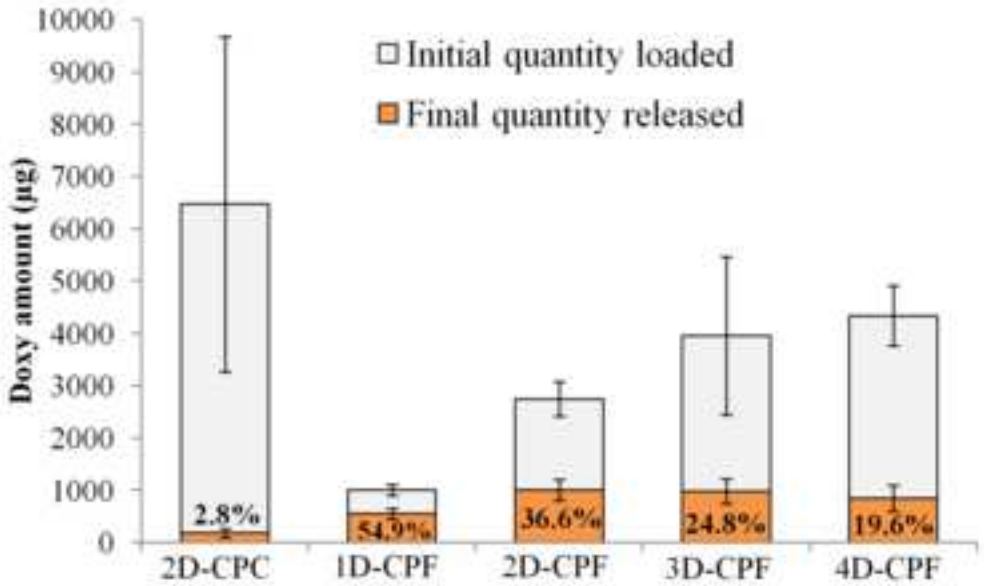

b)

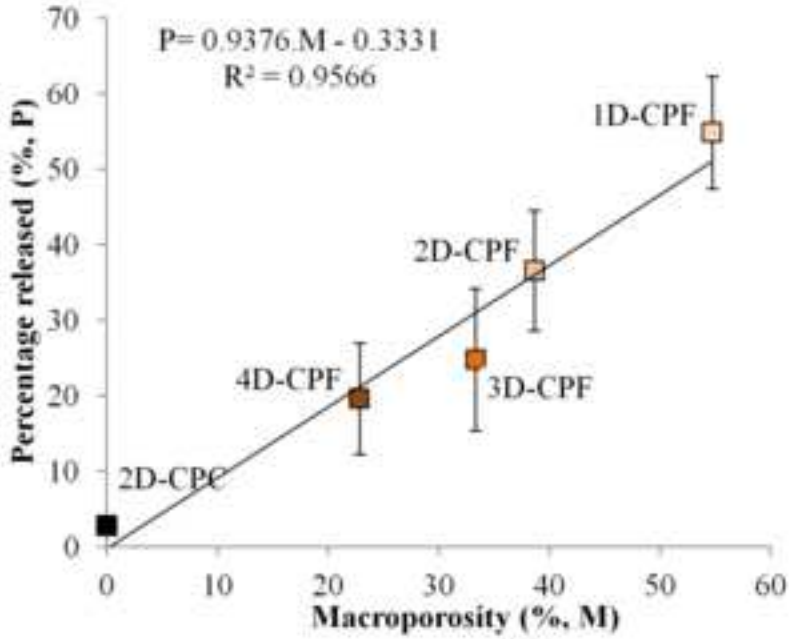

c)

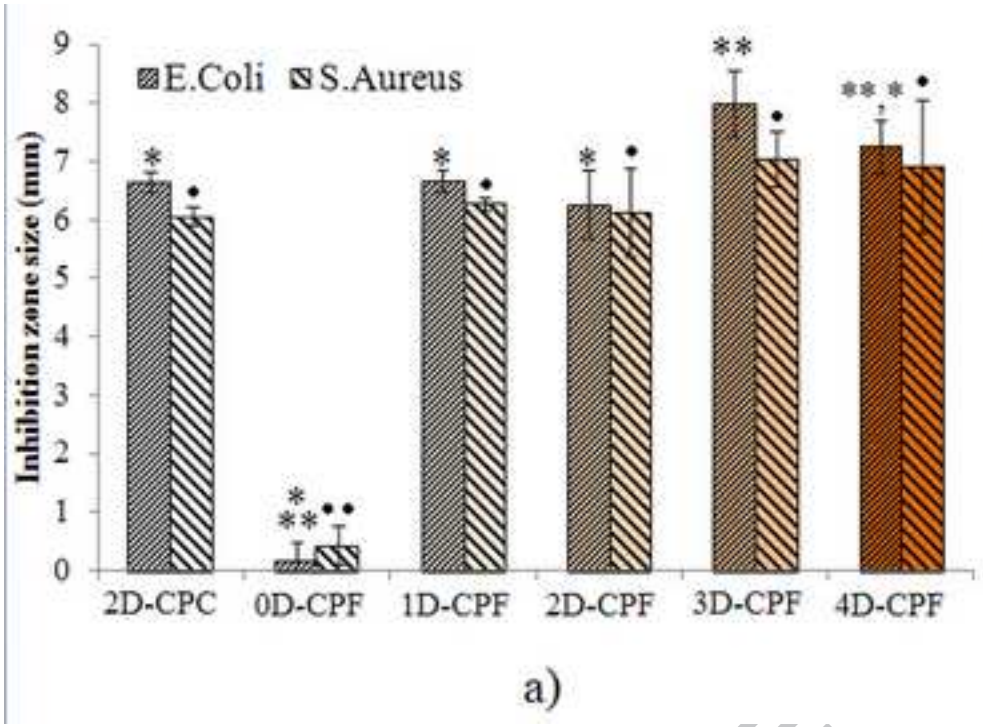

a)

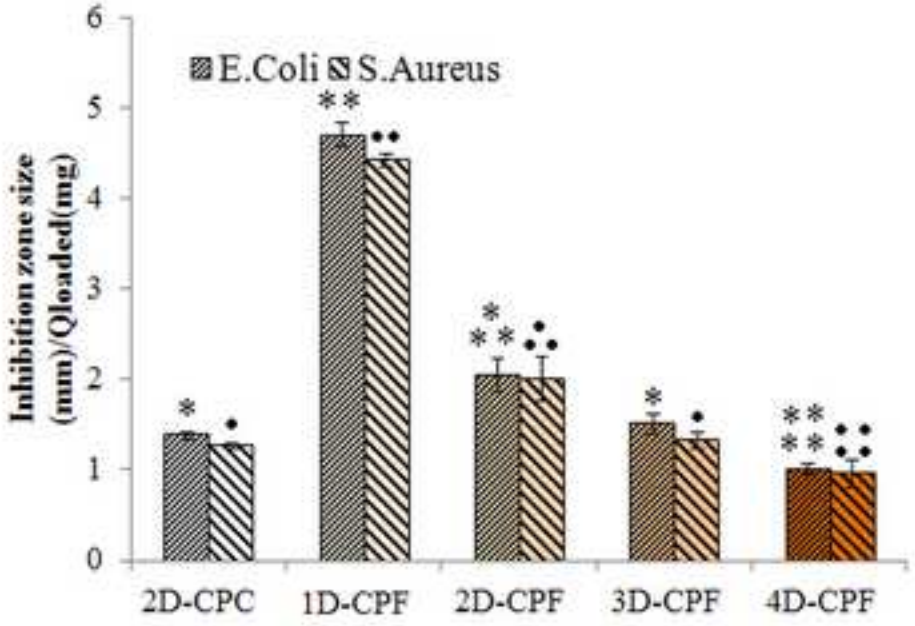

b)

Graphical Abstract

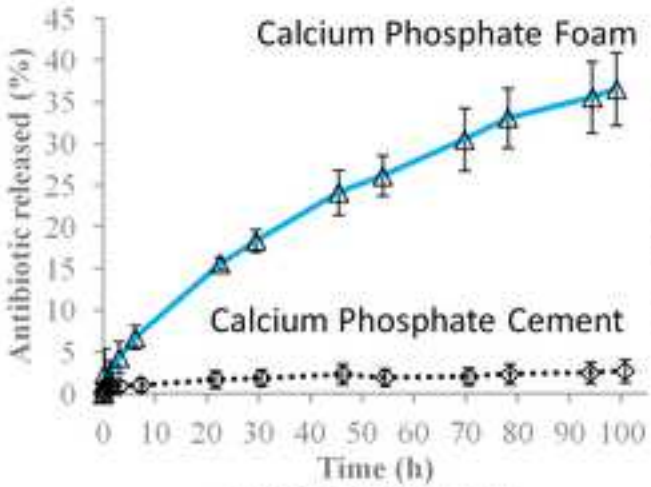

DRUG RELEASE

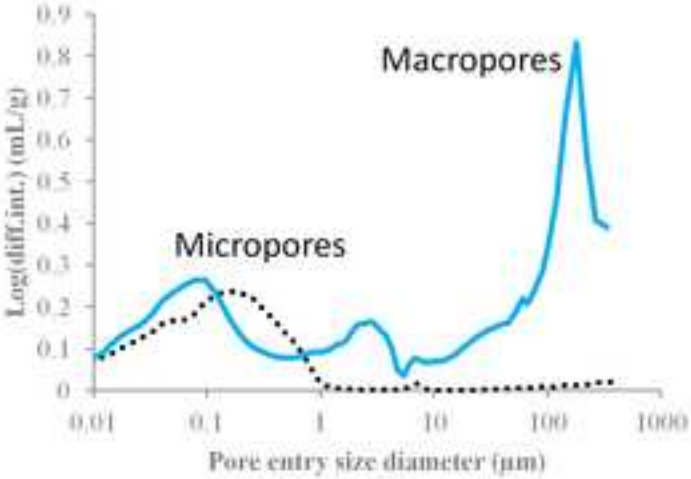

PORE ENTRY SIZE

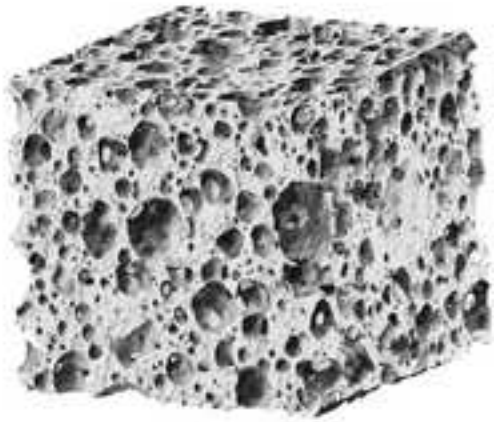

µCT